This article was downloaded by: [Yildiz Teknik University]
On: 02 September 2014, At: 01:00
Publisher: Taylor & Francis
Informa Ltd Registered in England and Wales Registered Number: 1072954 Registered office: Mortimer House, 37-41 Mortimer Street, London W1T 3JH, UK



Desalination and Water Treatment
Publication details, including instructions for authors and subscription information:
http://www.tandfonline.com/loi/tdwt20

Equilibrium and kinetic study on the adsorption of basic dye (BY28) onto raw Ca-bentonite

Yasemen Kalpaklı [a], Şafak Toygun [a], Gülhan Köneçoğlu [a] & Mesut Akgün [a]

[a] Chemical Engineering Department, Yildiz Technical University, Davutpasa Campus, No. 127, Esenler 34210, Istanbul, Turkey Phone: Tel. +90 212 383 4759, +90 212 383 4751 Fax: Tel. +90 212 383 4759, +90 212 383 4751

Published online: 23 Sep 2013.

To cite this article: Yasemen Kalpaklı, Şafak Toygun, Gülhan Köneçoğlu & Mesut Akgün (2013): Equilibrium and kinetic study on the adsorption of basic dye (BY28) onto raw Ca-bentonite, Desalination and Water Treatment, DOI: 10.1080/19443994.2013.830804

To link to this article: http://dx.doi.org/10.1080/19443994.2013.830804

PLEASE SCROLL DOWN FOR ARTICLE

Taylor & Francis makes every effort to ensure the accuracy of all the information (the "Content") contained in the publications on our platform. However, Taylor & Francis, our agents, and our licensors make no representations or warranties whatsoever as to the accuracy, completeness, or suitability for any purpose of the Content. Any opinions and views expressed in this publication are the opinions and views of the authors, and are not the views of or endorsed by Taylor & Francis. The accuracy of the Content should not be relied upon and should be independently verified with primary sources of information. Taylor and Francis shall not be liable for any losses, actions, claims, proceedings, demands, costs, expenses, damages, and other liabilities whatsoever or howsoever caused arising directly or indirectly in connection with, in relation to or arising out of the use of the Content.

This article may be used for research, teaching, and private study purposes. Any substantial or systematic reproduction, redistribution, reselling, loan, sub-licensing, systematic supply, or distribution in any form to anyone is expressly forbidden. Terms & Conditions of access and use can be found at http://www.tandfonline.com/page/terms-and-conditions

Desalination and Water Treatment
www.deswater.com
doi: 10.1080/19443994.2013.830804

(2013) 1–11

Taylor & Francis
Taylor & Francis Group

Equilibrium and kinetic study on the adsorption of basic dye (BY28) onto raw Ca-bentonite

Yasemen Kalpaklı*, Şafak Toygun, Gülhan Köneçoğlu, Mesut Akgün*

Chemical Engineering Department, Yildiz Technical University, Davutpasa Campus, No. 127, Esenler 34210, Istanbul, Turkey
Tel. +90 212 383 4759, +90 212 383 4751; Fax: +90 212 383 4725; emails: kalpakli@yildiz.edu.tr; akgunm@yildiz.edu.tr

Received 6 July 2012; Accepted 1 July 2013

Downloaded by [Yildiz Teknik University] at 01:00 02 September 2014

ABSTRACT

The adsorption of Basic Yellow 28 (BY28) onto bentonite in a batch system was carried out at temperatures of 20 and 40°C. The initial dye concentrations were in the range of 100 and 300 mg/L based on the total organic carbon (TOC) content of the dye solution. The effects of contact time, initial pH, and initial dye concentration on BY28 adsorption by the bentonite have been studied. BY28 removal was observed to increase until equilibrium, with increasing contact time and initial dye concentration, and the adsorption capacity of bentonite was seen to increase with increasing pH from 3 to 8. Adsorption efficiencies up to about 98.1% were obtained based on the TOC at various adsorption conditions. The adsorption process was determined to follow the pseudo-second-order adsorption kinetics. Kinetic parameters, rate constants, equilibrium adsorption capacities, and correlation coefficients of the adsorption kinetic models were calculated and discussed. The experimental isotherm data were analyzed using the Langmuir and Freundlich equations. The Langmuir isotherm represents that the adsorption of BY28 is indicating a very good mathematical fit compared with the Freundlich equation. The maximum monolayer adsorption capacity (q_{max}) of the Ca-bentonite was determined as 94.3396 mg/g for 20°C and 99.0295 mg/g for 40°C.

Keywords: Dye; Basic Yellow 28; Adsorption; Adsorption kinetics; Bentonite

1. Introduction

Synthetic dyes are widely used in the textile and biomedical or dyestuff industries for textile dyeing, paper printing, food, cosmetics, pharmaceutical, and color photography. On the other hand, synthetic dyes exhibit considerable structural diversity. The chemical classes of dyes employed more frequently on industrial scale are the azo, anthraquinone, sulfur, indigoid, triphenylmethyl(trityl), and phthalocyanine derivatives. Azo dyes are the most important group of synthetic colorant that are extensivelly used in textile, pharmaceutical, and printing industries [1]. But, the studies showed that the azo dyes and their subproducts may be carcinogenic and/or mutagenic [2]. Moreover, organic compounds and color are the main pollutants that make the treatment process difficult.

The direct discharge of textile wastewater into surface waters causes serious environmental problems by destroying many life forms, and consumes dissolved oxygen due to its strong color [3,4]. As a result of the aforementioned potential hazards and resulting environmental problems, many countries have forbidden

*Corresponding authors.

1944-3994/1944-3986 © 2013 Balaban Desalination Publications. All rights reserved.

Downloaded by [Yildiz Teknik University] at 01:00 02 September 2014

the direct discharge of textile wastewater into the environment. In consequence, a growing interest in the development of new technologies and procedures for the treatment of textile wastewater has emerged, including physicochemical and biological methods as well as the combinations thereof. Conventional methods of dyeing wastewater treatment include adsorption [5,6], flocculation [7], electrochemical methods [8–10], membrane separation [11], ozonation [7,12], advanced oxidation using UV/H_2O_2 or UV/TiO_2 [13–15], and biological oxidation [16–18]. Some other advanced oxidation methods for dyeing wastewater treatment are wet air oxidation [19] and supercritical water oxidation [20,21], which are performed at sub and supercritical temperatures and pressures of water, respectively. However, although they have very high treatment efficiencies in short reaction times, these technologies have disadvantages such as high capital cost and operational costs. Instead of the mentioned methods above, the adsorption technique can be applied to remove these kinds of textile effluents.

Adsorption offers significant advantages over traditional treatment methods, especially environmental point of view. Activated carbon is widely used as an adsorbent for dye removal from colored waters owing to its excellent adsorption properties, although it is high in price which limits their usage. More recently, interest has been shifted to alternative low-cost, novel, locally available adsorbents for the removal of textile dye effluents from aqueous solutions instead of activated carbon. For instance, clays such as bentonite (montmorillonite), nontronite, and saponite placed in smectite mineral group can be used in these respects [22,23]. Especially, bentonite provides an alternative because of its naturally available and unique physiochemical properties.

The layered structure of bentonite allows swelling after wetting, and Na^+ and Ca^{2+} are the hydrates in the presence of water. Therefore, since there is a hydrophilic environment at the clay surface, it is considered that natural bentonite is not an effective adsorbent for the nonpolar organic compounds in water. Mostly, after the surface properties of bentonite are changed by using modifiers, such as 1,6-diamino hexane, cetyltrimethylammonium bromide, some acids, and iron organo–inorgano pillars, bentonite is used as an adsorbent. In literature, there are many studies on the textile dyes obtained from aqueous solutions by adsorption onto modified bentonite [24–27]. However, there is a couple of study in this subject that uses natural bentonite, which is Na^+-bentonite [28–30]. In this study, removal of a commercial dye Basic Yellow 28 (BY28) from aqueous solution has been studied using natural Ca^{2+}-bentonite as an adsorption material. The monolayer equilibrium adsorption capacity was estimated using an adsorption isotherm technique. The effects of various adsorption conditions, such as initial dye concentration, amount of adsorbent used, temperature, and initial pH value of the dye solution, have been studied. The changes of bentonite surface properties induced by dye adsorption have been characterized by X-ray diffraction (XRD) and Scanning electron microscope (SEM) analyses.

2. Materials and methods

2.1. Materials

The natural bentonite used in this study was supplied from Kütahya, Turkey by ESSAN, and was crushed, ground, and sieved thought a sieve of 100 μm, and then dried at 100 °C in an incubator for 45 min before using in the experiments. The dried bentonite sample was stored in desiccators for using it in further experiments. Basic Yellow 28 (BY28) was kindly supplied by Alptekin Boya ve Kimyevi Maddeler AŞ with commercial name Cationic Gold Yellow X-GL 400%, and the stock solution of BY28 dye was prepared in 1,000 ppm concentration. All the chemicals used were of analytical reagent grade.

2.2. Experimental procedure

The removal of BY28 from aqueous solutions was carried out using bentonite as an adsorbent in a batch reactor. The effects of pH, amount of adsorbent, initial dye concentration, and contact time were investigated for the determination of optimum adsorption conditions. Desired amount of bentonite was contacted with a dye solution of 50 mL in a certain concentration of BY28 until the equilibrium time was reached. The system was stirred during the adsorption process at 480 rpm stirring speed. The initial pH of each solution was adjusted to the required value with 0.1 N HCl or 0.1 N NaOH solutions before mixing with bentonite. Then, the adsorption method given above was applied. All the kinetic experiments were conducted at 20 and 40 °C. After filtration of the solid phase, BY28 content in the liquid phase was determined by TOC. In order to determine the effect of Ca-bentonite on the color properties of water, absorbance values of each experiment were measured. Absorbance values were recorded at $\lambda_{max} = 438$ nm.

2.3. Analytical methods

Chemical composition of bentonite was determined using a Spectro-IQ2 type XRF spectrometry.

Downloaded by [Yildiz Teknik University] at 01:00 02 September 2014

XRF spectrometry is a technique used mainly for the analysis of materials because it requires relatively large amounts of sample (about 1 g). It can be used to measure all of the major elements in a mineral as well as a wide variety of trace elements. The samples were prepared to fine powder grinding the mineral for either pressing the powder into a pill or melting and quenching the sample to make a glass disk.

The surface area of bentonite was determined by nitrogen adsorption isotherms at 77 K measured by Quantachrome Autosorb Automated Gas Sorption System surface area analyzer using the Brunauer, Emmet, and Teller method. XRD experiments were conducted in a Rigaku™ RINT X using the settings of 40 mA and 30 kV at a 2θ range between 0° and 80°.

Major functional groups were analyzed by the Fourier transform infrared (FTIR) spectroscopy. Disks were prepared by mixing powdered bentonite with KBr in an agate mortar. The bentonite powder was mixed with KBr by a weight ratio of 1:1,500 approximately. After the mixture was provided to pellet by pressing under a pressure of 10 ton/cm^2 for 5 min, the spectra of the samples were recorded between 4,000 and 400 cm^{-1} using a Perkin–Elmer spectrum one spectrophotometer.

The potentiometric titration allows the determination of the chemical properties of materials by proton binding adsorption. Therefore, the potentiometric titrations of the bentonite were carried out using the method described by Helferrich [31]. A certain number of bentonite samples (75 mg each) were weighed into separate flasks, and were prepared by the addition of excessive amounts of 0.1 M NaOH or HCl to the different samples. About 10 mL of 0.1 M NaCI solution was added to each flask to keep a high background electrolyte concentration. Then, the total batch volume was observed to be 15 mL by the addition of distilled water to maintain the solution volume to sorbent weight ratio constant.

A blank experiment was also performed without using bentonite. After the batch was provided to reach equilibrium for 48 h, the equilibrium pH was measured for each sample. Basic titration data were transformed into proton-binding isotherms using a proton balance equation and theoretical blank reference. It was observed that the proton-binding isotherms obtained were positive for the proton-binding process and negative for proton dissociation.

SEM (JEOL-5410LV) with bath scatter electron detector and secondary electron detector was used to visualize the surface morphology and the structure of bentonite.

All the pH measurements were carried out with a pH-meter (WTW) and a combination of pH electrode. The analysis of the dyes used in this study was performed by a UV–vis Perkin–Elmer Lambda 35 spectrophotometer.

The concentrations of the model dye wastewater at initial stage and after adsorption process were characterized by the analyses of the total organic carbon (TOC) contents. TOC analyses were performed by TOC analyzer (HACH-LANGE IL550 TOC-TN), which is based on combustion catalytic oxidation method, using a highly sensitive multichannel nondispersive infrared detector. Standard solutions for calibration were prepared by using potassium hydrogen phthalate (Acros). All the reagents were pure for analytical use. In order to provide precise data, the samples were analyzed in triplicate, and the averages are reported as results.

3. Results and discussion

3.1. Material characteristics

The bentanite used in the experiments was characterized by using XRD, XRF, FTIR, and SEM measurements. The chemical composition of bentonite is given in Table 1. The mineral phases of bentonite were identified as montmorillonite ($2\theta = 5.73°$), cristobalite ($2\theta = 21.48°$), and anorthite ($2\theta = 28.032°$) as shown in Fig. 1. However, as can be seen in Fig. 1 and Table 2, montmorillonite structure does not change during the adsorption process; but after the adsorption, the intensity of peak increased with decreasing its basal spacing. As a result, cationic dye BY28 deposits onto the surface of clay layer and attaches to the edges of bentonite. On the other hand, the diffraction angle of bentonite (2θ) and the diffraction BY28-bentonite were obtained as 5.73 and 5.85, respectively, from X-ray patterns. This result shows that the diffraction peak of BY28-bentonite moves towards right. The XRD spectra

Table 1
Chemical composition of the bentonite

Component	Weight (%)
SiO_2	66.40
Al_2O_3	13.15
Fe_2O_3	0.69
TiO_2	0.02
CaO	4.18
MgO	3.5
Na_2O	0.13
K_2O	0.58
LOI*	11.25

*Loss ignition of bentonite.

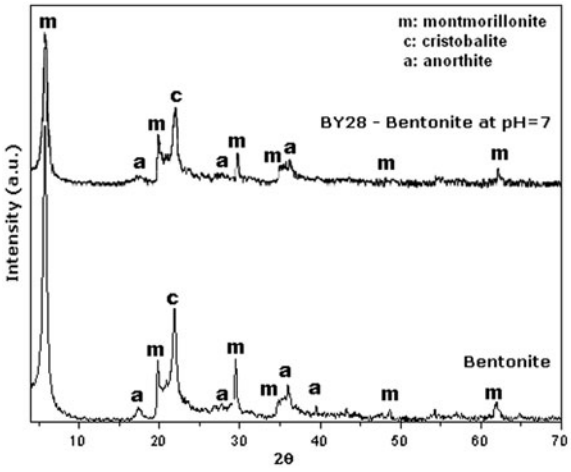


Fig. 1. The X-ray diffractogram of the bentonite and after adsorption of the bentonite.

of BY28-bentonite indicated that BY28 adsorption may lead to changes in unit cell dimensions and symmetry of the parent bentonite [32]. The specific surface area and cation exchange capacity of bentonite were 74.05 m^2/g and 95.20 meq/100 g, respectively.

FT-IR spectra of the bentonite are shown in Fig. 2 (a). The peaks between 3,500 and 3,700 cm^{-1} and near 3,400, 910, and 842 cm^{-1} indicated that this material is montmorillonite-rich smectite clay. The FTIR spectrum of the bentonite (Fig. 2(a)) exhibited major IR absorption bands at 3,626 cm^{-1} (Al–OH stretching), 3,398 cm^{-1} (OH stretching of adsorbed water), 1,632 cm^{-1} (OH bending of adsorbed water), 1,031 cm^{-1} (Si–O stretching), and 916 cm^{-1} (Al–OH bending), which are very close to those reported by Sakurai and Huang [33]. The Si–O–Al and Si–O–Mg bending vibrations were seen at 525 and at 473 cm^{-1}, respectively, which were also very close to those reported by Lou and Huang [34], and Sakurai and Huang [33]. The IR absorption bands at 794 and 672 cm^{-1} are characteristic to the mineral cristobalite, which was present in the bentonite as impurity [35,36]. In order to confirm the adsorption of dye molecules, FT-IR spectra of bentonite with the adsorped dye molecules at pH 7 and C.I. Basic Yellow 28 were taken and are shown in Fig. 2(b) and (c). Fig. 2(b) shows the characteristic peaks of the dye indicating the adsorption of dye on the bentonite. These peaks are at 1,557, 1,327, and 1,292 cm^{-1} due to the azo group of the dye.

The potentiometer titration allows the determination of the chemical properties of bentonite by proton binding adsorption. The pH titrations of bentonite were carried out using the method described by Helferrich [31]. As shown in Fig. 3, the surface of bentonite is neutral at pH 8.38, which is the intersection point of proton binding pH titration curve and pH axis. The pH value of the surface is called as *point of zero charge* (pH_{pzc}). The surface of the particle is positive at $pH < pH_{pzc}$, and is more attractive for anions. On the contrary, it is charged with negative and is more attractive for cations, since the acidic surface groups at the bentonite structure dissociate to its ions at $pH > pH_{pzc}$. However, although the dye BY28 used in this study has a cationic structure, the adsorption process is more efficient at values of $pH < pH_{pzc}$. Therefore, it can be said that the adsorption process is more effective than ion exchange in this study.

Table 2
Structure of the bentonite and after adsorption of the bentonite

Bentonite			BY28-bentonite at pH = 7		
Angle 2-theta°	Basal spacing (nm)	Intensity (%)	Angle 2-theta°	Basal spacing (nm)	Intensity (%)
5.729	15.41456	100.0	5.848	15.09959	100.0
17.373	5.10034	7.7	—	—	—
19.802	4.47996	22.9	19.885	4.46148	36.5
21.919	4.05179	40.0	22.001	4.03683	52.4
29.516	3.02394	22.9	29.632	3.01235	25.1
34.809	2.57529	11.1	34.923	2.56710	17.8
35.929	2.49748	14.9	35.592	2.52041	18.7
39.479	2.28073	7.7	—	—	—
43.215	2.09181	7.4	43.389	2.08380	9.2
48.632	1.87070	6.6	48.625	1.87096	9.7
54.174	1.69168	6.9	54.474	1.68310	19.2
61.833	1.49924	9.7	61.993	1.49577	15.0

Downloaded by [Yildiz Teknik University] at 01:00 02 September 2014

Downloaded by [Yildiz Teknik University] at 01:00 02 September 2014

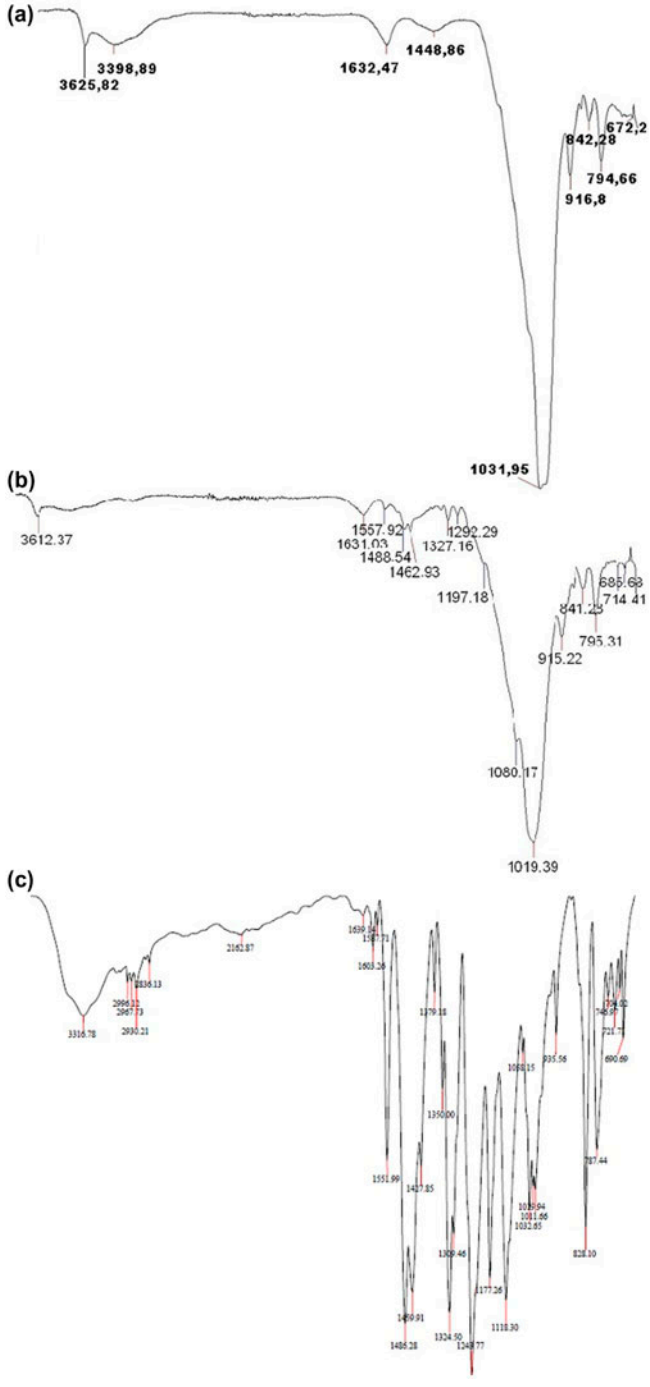


Fig. 2. The FT-IR spectrum of the bentonite.

3.2. *Adsorption studies of BY28 onto the Ca^{2+}-bentonite*

The adsorption experiments of BY28 onto the bentonite were performed based on the TOC removal in a batch reactor at 20 and 40°C. The initial TOC concentrations of BY28 ranged from 100 to 300 mg/L, and the experiments were carried out using the bentonite concentration of 100 mg/L. Equilibrium reaction time which shows maximum dye adsorption under the experimental condition was determined as 25 min at 100 ppm initial dye concentration. The most TOC removal was obtained as 98.1% at the initial TOC concentration of 100 mg/L. The results of the experiments show that BY28 in the aqueous solution was almost completely removed based on the TOC. As a result of

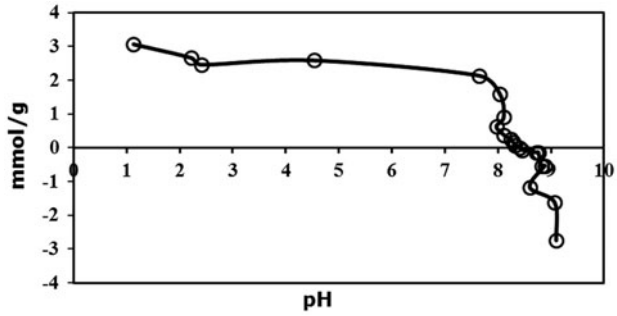


Fig. 3. The proton binding pH titration curve of the Ca-bentonite.

the adsorption process, a clear and colorless solution was obtained. Fig. 4(a) and (b) show the SEM images of bentonite before and after BY28 adsorption, respectively. It is observed that the bentonite in a stratum form is transform into lumped form after the adsorption process. This changing of the shape may be due to Na^+ and Ca^{2+} in the intralayer of bentonite which transforms into hydrate form because of getting wet, or the adsorption of BY28.

3.2.1. Effect of pH on the retention of BY28

In order to optimize the sorption conditions for the retention of BY28 on bentonite, the retention of BY28 was determined by applying the general sorption procedure by changing the pH of the sample solution in the range of 3 to 8. This sorption study was carried out at BY28 concentration of 100 ppm, bentonite amount of 0.1 g, and contact time of 25 min. As can be seen in Fig. 5, the highest quantitative retention of BY28, which is 31.921 mg/g (94.14%), is obtained at the pH 7.0. This situation shows that adsorption mechanism of BY28 on Kütahya-bentonite is controlled by the pH. Similar result has been reported for the adsorption of basic dye from aqueous solution onto bentonite [24,37,38]. On the other hand, Turabik [30] observed that adsorption mechanism of BY28 on Ordu-bentonite is advanced, independently of pH.

3.2.2. Effect of adsorbent doses

The effect of adsorbent dose was studied by bentonite mass that varied from 10 to 100 mg/L at pH 7 and a fixed initial dye concentration of 100 mg/L for 25 min. The general trend indicates that the adsorption of BY28 increases with increasing the adsorbent dose from 10 to 100 mg/L. As seen in Fig. 6, the equilibrium concentration of BY26 in the aqueous solution decreases with the adsorbent dose. At the adsorbent dose of 100 mg/L, removal efficiencies of 95% were observed. The increment of the removal efficiency is due to the increase of adsorbent dose that indicates an increase of the total available surface area of the adsorbent particles.

3.2.3. Effect of temperature

Effect of temperature on the removal of BY28 was performed at two different temperatures, i.e. 20 and 40°C. As shown in Fig. 7, the adsorption capacity of BY28 on bentonite is not affected by the temperature of the solution, when it increases from 20 to 40°C. However, the adsorption rate of BY28 on bentonite at 40°C is higher than that at 20°C at low initial dye concentrations (Fig. 7). This situation explains that the sorption of BY28 in high temperatures is faster than that in low temperatures, due to the mobility of the BY28 molecules which increases with an increase in temperature. Therefore, it is revealed that the process is endothermic. It is also observed in Table 3 that when the solution temperature increases from 20 to

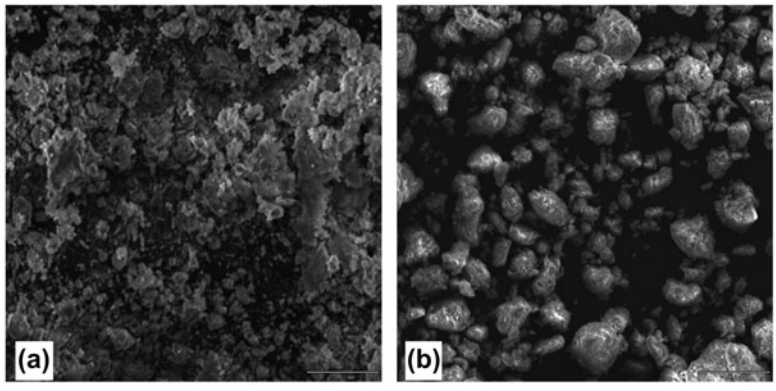


Fig. 4. SEM images of the Ca-bentonite: (a) before adsorption and (b) after BY28 adsorption.

Downloaded by [Yildiz Teknik University] at 01:00 02 September 2014

Downloaded by [Yildiz Teknik University] at 01:00 02 September 2014

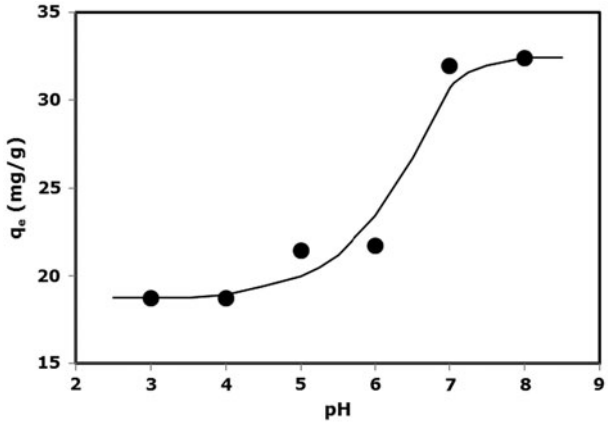


Fig. 5. The effect of pH on the retention of BY28 on the bentonite.

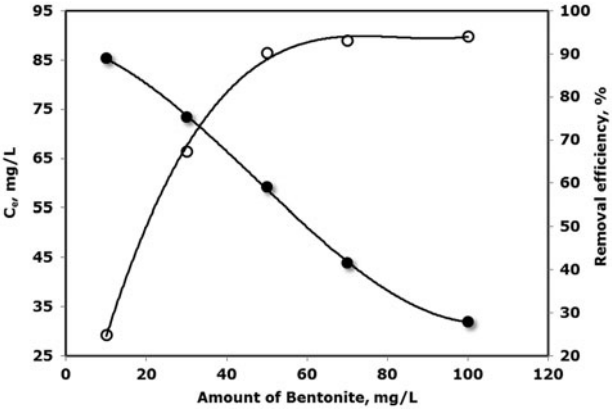


Fig. 6. The effect of absorbent mass used on BY28 absorption.

40 °C, the rate constant, k_2 increases from 3.042×10^{-3} to 0.041 g/mg min at the initial BY28 concentration of 100 mg/L (Table 3). However, this increment reduces with increasing the initial BY28 concentration.

3.2.4. Effect of concentration

To evaluate the sorption characteristics of bentonite for BY28, the change of sorption capacity with time for different initial solution concentrations has been investigated. A series of experiments were undertaken by varying the initial BY28 concentration in the range 100–300 mg/L on the removal kinetics of BY28 from the solution. Fig. 7 also shows that the adsorption of BY28 by bentonite increases as the initial BY28 concentration increase. Required contact time to reach equilibrium the BY28 solution was observed to be within 25 min at 100 and 200 ppm

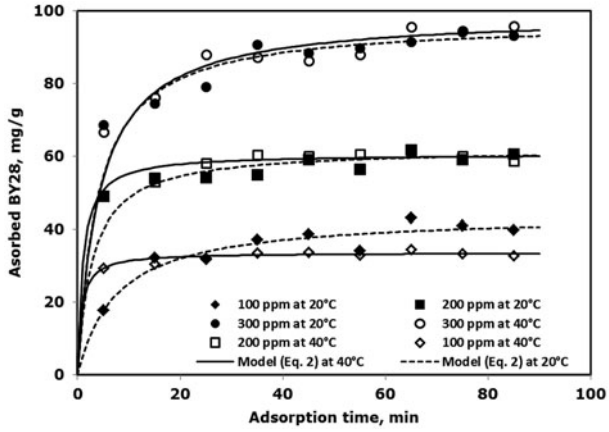


Fig. 7. The change of sorption capacity with time at various the initial BY28 concentrations.

initial dye concentration. However, the experimental data were measured up to 85 min to confirm the complete equilibrium reached at 300 ppm. It demonstrated that the concentration of dye is important depend on equilibrium contact time. At low dye concentrations, vacant surface sites adsorbed the dye more rapidly. One explanation for this observation may be the fact that at low concentration almost all the dye molecules are adsorbed very quickly on the outer surface. Further increase in the initial dye concentration led to fast saturation of adsorbent and thus, most of the dye adsorption took place slowly inside the pores by intraparticle diffusion. Steric repulsion between molecules of the solute can also minimize the adsorption process [39,40].

3.3. The kinetics of BY28 adsorption onto the bentonite

The adsorption kinetic data of BY28 were analyzed using two kinetics models, which were the pseudo-first order and the pseudo-second order equations. Lagergren [41] suggests the pseudo-first-order kinetics rate equation, and integrated the rate equation by applying the initial conditions as below:

$$\log(q_e - q_t) = \log q_e - \left(\frac{k_1}{2.303}\right)t \quad (1)$$

where q_e and q_t both (mg/g) are the amount of BY28 adsorbed per unit of mass of bentonite at equilibrium and time t, respectively, and k_1 is the pseudo-first-order rate constant (min^{-1}). In other words, q_e represents the adsorption capacity. The value for the k_1 was calculated from the slope of the linear plot of log ($q_e - q_t$) vs. t (Fig. 8). The k_1 values and correlation coefficients R^2 are given in Table 3. As shown in

Downloaded by [Yildiz Teknik University] at 01:00 02 September 2014

Fig. 8, pseudo-first-order kinetic model is not satisfactory for the adsorption of BY28 onto the bentonite.

The pseudo-second-order reaction rate equation was used by Ho et al. [42] to study the kinetics of adsorption of heavy metals on peat. This model was also applied to assess the kinetics of adsorption of BY28 on the bentonite. The pseudo-second-order rate kinetics are expressed as follows:

$$q_t = \frac{k_2 q_e^2 t}{1 + k_2 q_e t} \quad (2)$$

Linearized form of Eq. (2) can be described in linearized form as follows:

$$\frac{t}{q_t} = \frac{1}{k_2 q_e^2} + \frac{1}{q_e} t \quad (3)$$

where q_e and q_t both (mg/g) are the amount of BY28 adsorbed per unit of mass of the bentonite at equilibrium and time t, respectively, and k_2 is the rate constant of pseudo-second-order adsorption (g/mg min).

The kinetics plots between (t/q_t) vs. (t) were plotted for the different initial concentrations (Fig. 9(a) and (b)). Slope and intercept values were solved to give the value of pseudo-second-order rate constant (Table 3). Fig. 9(a) and (b), and Table 3 show that highly significant regression line ($r^2 > 0.97$) and the data were well fitted only to the pseudo-second-order rate equation (Figs. 7 and 9(a) and (b)). The straight line was obtained indicating that the process follow a pseudo-second-order kinetics for various concentration of BY28. While the initial BY28 concentration increases from 100 to 300 mg/L, the adsorption capacity (q_e) increase from 44.053 to 97.087 mg/g at 20°C and from 33.670 to 99.010 mg/g at 40°C. This indicates that the initial BY28 concentration plays a key role in determining the adsorption capacity of BY28 on the bentonite. It is also observed in Table 3 that when initial BY28 concentration increases from 100 to 300 mg/L, the rate constant, k_2 decreases from 3.042×10^{-3} to 2.652×10^{-3} g/mg min at 20°C and from 0.041 to 2.435×10^{-3} g/mg min at 40°C. Although the adsorption capacity (q_e) increases with increasing the initial dye concentration, k_2 reduces. The reason is that the adsorption process is slower to reach increased adsorption capacity (q_e) with increasing the initial dye concentration as seen in Fig. 7. In other words, while it is reached to the adsorption capacity in a short time at the low initial dye concentrations, on the contrary, it takes for a long time to reach to the adsorption capacity at the higher initial dye concentrations. In addition, the values of initial sorption rate, which is described as $h = k_2 q_e^2$, also increase from 5.903 to 25 mg/g.min at 20°C, and from 46.296 to 62.50 mg/g.min at 40°C. Fig. 10 shows a comparison between the experimental and predicted (Eq. 2) amount of BY28 adsorbed with increasing contact time. The dashed lines, indicating 95% confidence interval on the 45° line, contain all of the data point.

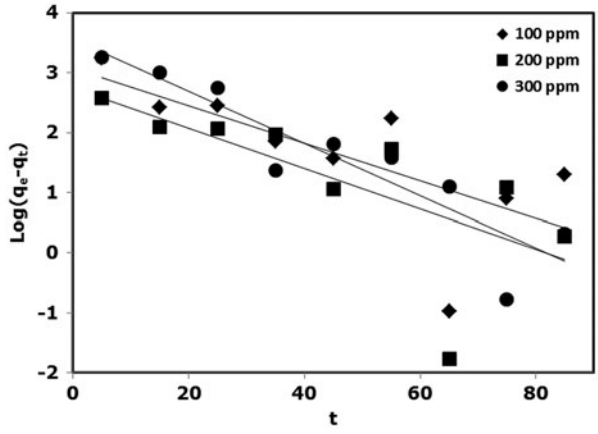


Fig. 8. Kinetics analysis of BY28 adsorption by linear plots of pseudo-first-order rate equation at 20°C.

3.4. Adsorption isotherm

The equilibrium adsorption isotherm is of importance in the design of adsorption systems [43].

Table 3
Kinetic parameters for the adsorption of BY28 onto bentonite at temperatures of 20 and 40°C

Temperature	Concentration	Pseudo-first-order model			Pseudo-second-order model		
(°C)	(mg/L)	k_1, (min^{-1})	q_e, (mg/g)	r^2	k_2, (g/mg min)	q_e, (mg/g)	r^2
20	100	0.031	21.693	0.909	3.042×10^{-3}	44.053	0.9798
20	200	0.034	15.502	0.914	3.022×10^{-3}	62.112	0.9963
20	300	0.041	35.023	0.927	2.652×10^{-3}	97.087	0.998
40	100	0.027	3.963	0.87	0.041	33.670	0.9982
40	200	0.037	7.272	0.924	0.017	60.606	0.9984
40	300	0.079	94.066	0.936	2.435×10^{-3}	99.010	0.9961

Downloaded by [Yildiz Teknik University] at 01:00 02 September 2014

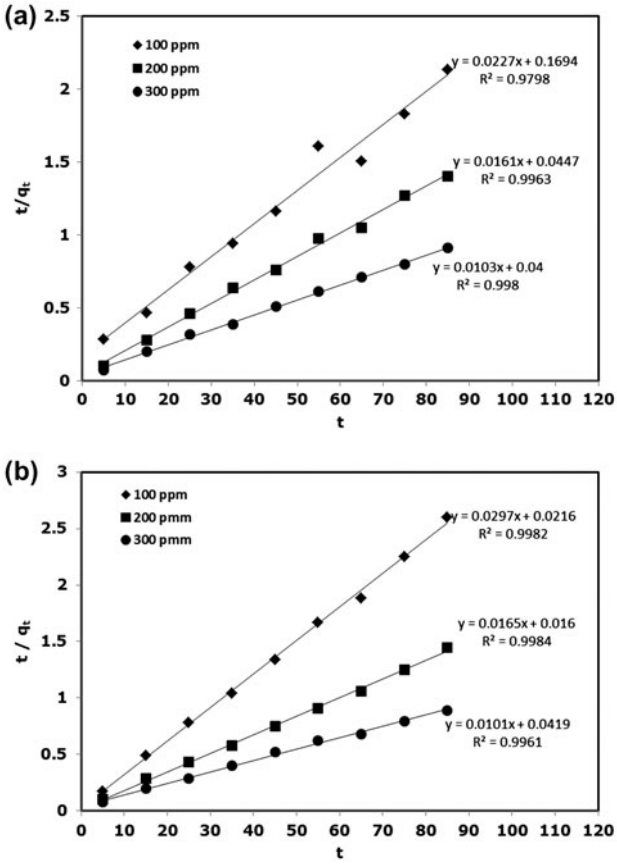


Fig. 9. Kinetics analysis of BY28 adsorption by linear plots of pseudo-second-order rate equations: (a) at 20˚C and (b) at 40˚C.

Although several isotherm equations are available in the literature, the Langmuir isotherm and the Freundlich isotherm are selected and tested in this study. The Freundlich isotherm is the earliest known relationship describing the adsorption isotherm. This fairly satisfactory empirical isotherm can be used in the adsorption from dilute solutions. The ordinary adsorption isotherm is expressed by the following equation:

$$q_e = K_F C_e^{1/n} \tag{4}$$

where C_e is the equilibrium concentration in the solution (mg/L), q_e the equilibrium adsorption capacity mg/g, and (K_F) and n are Freundlich constants related to adsorption capacity and adsorption intensity, respectively.

On applying the linearized form of Eq. (4) to the experimental data, the Freundlich model constants and r^2 values were obtained and are presented in Table 4. The Freundlich adsorption capacity (K_F) was found to be 32.5247 and 24.4102, and n which indicate

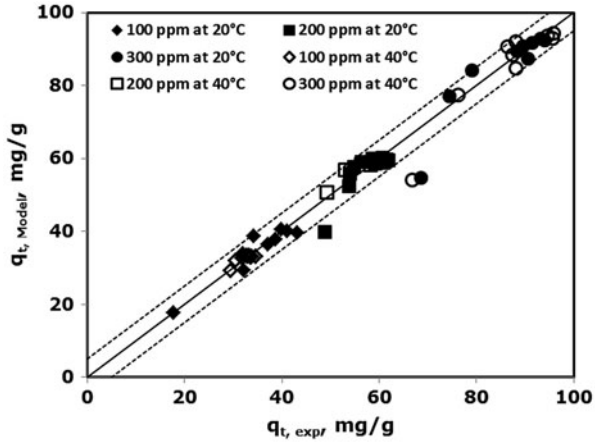


Fig. 10. A comparison of experimental data with predicted data (Eq. 4).

adsorption intensity was calculated as 4.065 and 2.924 for the temperatures of 20 and 40˚C, respectively (Table 4). In addition, the Freundlich adsorption isoterms of 20 and 40˚C are shown in Fig. 11.

The Langmuir adsorption isotherms assumes that adsorption takes place at specific homogeneous sites within the adsorbent and has found to have successful application to many sorption process of monolayer adsorption. The Langmuir adsorption isotherm can be written as:

$$q_e = \frac{K_L q_{max} C_e}{1 + K_L C_e} \tag{5}$$

The Langmuir parameters were obtained by fitting the experimental data to the linearized equation derived from Eq. (5):

$$\frac{c_e}{q_e} = \frac{1}{K_L q_{max}} + \frac{C_e}{q_{max}} \tag{6}$$

where q_e is the adsorbed amount mg/g of the BY28, C_e is the equilibrium concentration of the BY28 in solution mg/L, q_{max} is the maximum monolayer adsorption capacity mg/g, and K_L is the adsorption equilibrium constant. Based on Eq. (6), the isotherms were fitted to the adsorption data obtained. The Langmuir adsorption exponents for Eq. (6), the q_{max}, and K_L are determined from the linear plots of C_e/q_e vs. C_e, and the calculated correlation coefficients for these isotherms are shown in Table 4. The values of the Langmuir constant were calculated from the slopes and intercepts of the plots. The magnitude of Langmuir constant K_L is 0.1599 Lmg^{-1} for 20˚C and 0.1429 L/mg for 40˚C, and the maximum monolayer

Table 4
Parameters for the adsorption isotherm of BY28 onto bentonite

T (℃)	Langmuir isotherm			Freundlich isotherm		
	K_L (L mg^{-1})	q_{max} (mg/g)	r^2	K_F (L/g)	n	r^2
20	0.1599	94.3396	0.9970	32.5247	4.065	0.9916
40	0.1429	99.0295	0.9786	24.4102	2.924	0.6975

adsorption capacity (q_{max}) of the Ca-bentonite was determined as 94.3396 mg/g for 20℃ and 99.0295 mg/g for 40℃. As shown in Table 4 and Fig. 11, the Langmuir equation represents the adsorption process is very well and the correlation coefficient, R^2 value is indicating a very good mathematical fit compared with the Freundlich equation.

In order to predict the adsorption efficiency of the adsorption process, the dimensionless equilibrium parameter R_L was determined by using the following equation [42]:

$$R_L = \frac{1}{1 + K_L C_0} \tag{7}$$

where C_0 is the initial concentration and K_L is the Langmuir isotherm constant. The parameter R_L indicates the shape of isotherm. The process is irreversible if $R_L = 0$, favorable if $R_L < 1$, linear if $R_L = 1$, and unfavorable if $R_L > 1$. According to Eq. (7), it was obtained that the adsorption of BY28 onto the bentonite is a favorable process.

4. Conclusion

The adsorption of Basic Yellow 28 dye, which is a model wastewater, onto the Ca-bentonite was investigated in a batch system at pH 7.0 for temperatures of 20 and 40℃. It was observed that the Ca-bentonite had a high adsorption capacity for BY28 dye, and the most TOC removal was obtained as 98.1% at the initial TOC concentration of 100 mg/L. It was found that the kinetics of the adsorption of BY28 onto the bentonite at different initial concentrations was best described by the pseudo-second-order model. The Langmuir and Freundlich isotherm models applied to the experimental adsorption data of BY28 dye onto the bentonite. The Langmuir model agreed reasonably with the experimental adsorption data. The maximum monolayer adsorption capacity of the Ca-bentonite was determined as 94.3396 mg/g for 20℃ and 99.0295 mg/g for 40℃. Based on the results, it was concluded that the bentonite had a significant potential for removing basic dye from wastewater using adsorption method.

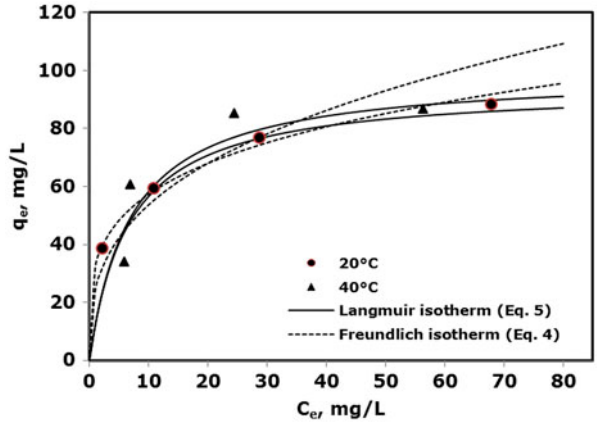


Fig. 11. Adsorption isotherms of BY28 onto bentonite.

Acknowledgments

This work has been supported by Yildiz Technical University, Scientific Research Projects Council (YTU-BAPK, project no: 2011-07-01-KAP04).

References

[1] E. Forgacs, T. Cserhatia, G. Oros, Removal of synthetic dyes from wastewaters: A review, Environ. Int. 30 (2004) 953–971.
[2] N. Puvaneswari, P. Muthukrishnan, P. Gunasekaran, Toxicity assessment and microbial degradation of azo dyes, Indian J. Exp. Biology 44 (2006) 618–626.
[3] P.C. Vandevivere, R. Bianchi, W. Verstraete, Treatment and reuse of wastewater from the textile wet-processing industry: Review of emerging technologies, J. Chem. Technol. Biotechnol. 72 (1998) 289–302.
[4] C. O'Neill, F. Hawkes, D. Hawkes, N. Lourenco, H. Pinheiro, W. Delee, Colour in textile effluents-sources, measurement, discharge consents and simulation: A review, J. Chem. Technol. Biotechnol. 74 (1999) 1009–1018.
[5] H.K. Can, B. Kirci, S. Kavlak, A. Guner, Removal of some textile dyes from aqueous solutions by poly(N-vinyl-2-pyrrolidone) and poly(N-vinyl-2-pyrrolidone)/$K_2S_2O_8$ hydrogels, Radiat. Phys. Chem. 68 (2003) 811–818.
[6] L.C. Morais, O.M. Freitas, E.P. Gonçalves, L.T. Vasconcelos, C.G. Gonzalez Beça, Reactive dyes removal from wastewaters by adsorption on eucalyptus bark: Variables that define the process, Water Res. 33 (1999) 979–988.
[7] G. Ciardelli, N. Ranieri, The treatment and reuse of wastewater in the textile industry by means of ozonation and electroflocculation, Water Res. 35 (2001) 567–572.

Downloaded by [Yildiz Teknik University] at 01:00 02 September 2014

Downloaded by [Yildiz Teknik University] at 01:00 02 September 2014

[8] L. Szpyrkowicz, C. Juzzolino, S.N. Kaul, A comparative study on oxidation of disperse dyes by electrochemical process, ozone, hypochloride and fenton reagent, Water Res. 35 (2001) 2129–2136.

[9] A.G. Vlyssides, D. Papaioannou, M. Loizidoy, P.K. Karlis, A.A. Zorpas, Testing an electrochemical method for treatment of textile dye wastewater, Waste Manage. 20 (2000) 569–574.

[10] Y. Xiong, P.J. Strunk, H. Xia, X. Zhu, H.T. Karlsson, Treatment of dye wastewater acid orange II using a cell with three-phase three-dimensional electrode, Water Res. 35 (2001) 4226–4230.

[11] X. Tan, N.N. Kyaw, W.K. Teo, K. Li, Decolorization of dye-containing aqueous solutions by the polyelectrolyte-enhanced ultrafiltration (PEUF) process using a hollow fiber membrane module, Sep. Purif. Technol. 52 (2006) 110–116.

[12] S. Dogruel, E. Dulekgurgen, D. Orhon, Effect of ozonation on chemical oxygen demand fractionation and color profile of textile wastewaters, J. Chem. Technol. Biotechnol. 81 (2006) 426–432.

[13] E. Kusvuran, O. Gulnaz, S. Irmak, O.M. Atanur, H.I. Yavuz, O. Erbatur, Comparison of several advanced oxidation processes for the decolorization of reactive red 120 azo dye in aqueous solution, J. Hazard. Mater. B109 (2004) 85–93.

[14] B. Ulusoy, E. Catalkaya, F. Sengul, Photodegradation of reactive black 5, direct red 28 and direct yellow 12 using UV, UV/H_2O_2 and $UV/H_2O_2/Fe^{2+}$: A comparative study, J. Hazard. Mater. B114 (2004) 159–166.

[15] C. Tang, V. Chen, The photocatalytic degradation of reactive black 5 using TiO_2/UV in an annular photoreactor, Water Res. 38 (2004) 2775–2781.

[16] S.M. Ghoreishi, R. Haghighi, Chemical catalytic reaction and biological oxidation for treatment of non-biodegradable textile effluent, Chem. Eng. J. 95 (2003) 163–169.

[17] U. Zissi, G. Lyberatos, Azo-dye biodegradation under anoxic conditions, Water. Sci. Technol. 34 (1996) 495–500.

[18] J.S. Knapp, P.S. Newby, L.P. Reece, Decolorization of dyes by woodrotting basidiomycete fungi, Enzyme Microb. Technol. 17 (1995) 664–668.

[19] J. Donlagic, J. Levec, Oxidation of an azo dye in subcritical aqueous solutions, Ind. Eng. Chem. Res. 36 (1997) 3480–3486.

[20] O.Ö. Söğüt, M. Akgün, Treatment of textile wastewater by SCWO in a tube reactor, J. Supercrit. Fluids 43 (2007) 106–111.

[21] O.Ö. Söğüt, M. Akgün, Treatment of dyehouse waste-water by supercritical water oxidation: A case study, J. Chem. Technol. Biotechnol. 85 (2010) 640–647.

[22] O. Ozdemir, B. Armagan, M. Turan, M.S. Çelik, Comparison of the adsorption characteristics of azo-reactive dyes on mezoporous minerals, Dyes Pigm. 62 (2004) 49–60.

[23] E. Eren, Investigation of a basic dye removal from aqueous solution onto chemically modified unye bentonite, J. Hazard. Mater. 166 (2009) 88–93.

[24] Ö. Gök, A.S. Özcan, A. Özcan, Adsorption behavior of a textile dye of reactive blue 19 from aqueous solutions onto modified bentonite, Appl. Surf. Sci. 256 (2010) 5439–5443.

[25] L. Zhu, J. Ma, Simultaneous removal of acid dye and cationic surfactant from water by bentonite in one-step process, Chem. Eng. J. 139 (2008) 503–509.

[26] F. Zermane, O. Bouras, M. Baudu, J.P. Basly, Cooperative coadsorption of 4-nitrophenol and basic yellow 28 dye onto an iron organo–inorgano pillared montmorillonite clay, J. Col. Int. Sci. 350 (2010) 315–319.

[27] M. Hajjaji, H. El Arfaoui, Adsorption of methylene blue and zinc ions on raw and acid-activated bentonite from Morocco, Appl. Clay Sci. 46 (2009) 418–421.

[28] A.S. Özcan, B. Erdem, A. Özcan, Adsorption of acid blue 193 from aqueous solutions onto Na–bentonite and DTMA–bentonite, J. Col. Int. Sci. 280 (2004) 44–54.

[29] M. Turabik, Adsorption of basic dyes from single and binary component systems onto bentonite: Simultaneous analysis of basic red 46 and basic yellow 28 by first order derivative spectrophotometric analysis method, J. Hazard. Mater. 158 (2008) 52–64.

[30] S. Hong, C. Wen, J. He, F. Gan, Y.S. Hob, Adsorption thermodynamics of methylene blue onto bentonite, J. Hazard. Mater. 167 (2009) 630–633.

[31] F. Helferrich, Ion Exchange, Dover Pub., New York, NY, 1995.

[32] E. Eren, B. Afsin, Investigation of a basic dye adsorption from aqueous solution onto raw and pre-treated bentonite surfaces, J. Hazard. Mater. 151 (2008) 682–691.

[33] K. Sakurai, P.M. Huang, Intercalation of hydroxy-aluminosilicate and hydroxy-aluminum in montmorillonite and resultant physicochemical properties, Soil Sci. Soc. Am. J. 62 (1998) 362–368.

[34] G.Q.J. Lou, P.M. Huang, Interlayer adsorption of polymeric hydroxy-aluminosilicate ions by montmorillonite, Soil Sci. Soc. Am. J. 58 (1994) 745–750.

[35] H.W.V. Marel, H. Beutelspacher, Atlas of infrared spectroscopy of clay minerals and their admixtures, Elsevier Sci. Pub. Commun., Amsterdam, 1976.

[36] K. Inoue, C. Satoh, Surface-charge characteristics of hydroxyaluminosilicate and hydroxyaluminum montmorillonite complexes, Soil Sci. Soc. Am. J. 57 (1993) 545–552.

[37] G. McKay, G. Ramprasad, P.P. Mowli, Equilibrium studies for the adsorption of dyestuffs from aqueous solutions by low-cost materials, Water Air Soil Pollut. 29 (1986) 273–283.

[38] B. Cheknane, O. Bouras, M. Baudu, J.P. Basly, A. Cherguielaine, Granular inorgano-organo pillared clays (GIOCs): Preparation by wet granulation, characterization and application to the removal of a basic dye (BY28) from aqueous solutions, Chem. Eng. J. 158 (2010) 528–534.

[39] B.H. Hameed, Equilibrium and kinetic studies of methyl violet sorption by agricultural waste, J. Hazard. Mater. 154 (2008) 204–212.

[40] B.H. Hameed, M.I. El-Khaiary, Removal of basic dye from aqueous medium using a novel agricultural waste material: Pumpkin seed hull, J. Hazard. Mater. 155 (2008) 601–609.

[41] S. Lagergren, Zur theorie der sogenannten adsorption geloster stoffe [The theory of so-called adsorption of dissolved substances], Kungliga Svenska Vetenskapsakademiens, Handlingar 24 (1898) 1–39.

[42] Y.S. Ho, D.A.J. Wase, C.F. Forster, Kinetic studies of competitive heavy metal adsorption by sphagnum moss peat, Environ. Technol. 17 (1996) 71–77.

[43] Y.H. Magdy, A.A.M. Daifullah, Adsorption of a basic dye from aqueous solutions onto sugar-industry-mud in two modes of operations, Waste Manage. 18 (1988) 219–226.